

# Multi-order Graph Clustering with Adaptive Node-level Weight Learning

Ye Liu<sup>a,\*</sup>, Xuelei Lin<sup>b</sup>, Yejia Chen<sup>a</sup>, Reynold Cheng<sup>c</sup>

<sup>a</sup>*School of Future Technology, South China University of Technology, Guangzhou, China*

<sup>b</sup>*School of Science, Harbin Institute of Technology, Shenzhen, China*

<sup>c</sup>*Department of Computer Science, The University of Hong Kong, Hong Kong, China*

---

## Abstract

Current graph clustering methods emphasize individual node and edge connections, while ignoring higher-order organization at the level of motif. Recently, higher-order graph clustering approaches have been designed by motif-based hypergraphs. However, these approaches often suffer from hypergraph fragmentation issue seriously, which degrades the clustering performance greatly. Moreover, real-world graphs usually contain diverse motifs, with nodes participating in multiple motifs. A key challenge is how to achieve precise clustering results by integrating information from multiple motifs at the node level. In this paper, we propose a multi-order graph clustering model (MOGC) to integrate multiple higher-order structures and edge connections at node level. MOGC employs an adaptive weight learning mechanism to automatically adjust the contributions of different motifs for each node. This not only tackles hypergraph fragmentation issue but enhances clustering ac-

---

\*Corresponding author

*Email addresses:* yliu03@scut.edu.cn (Ye Liu), linxuelei@hit.edu.cn (Xuelei Lin), 202221062461@mail.scut.edu.cn (Yejia Chen), ckcheng@cs.hku.hk (Reynold Cheng)

curacy. MOGC is efficiently solved by an alternating minimization algorithm. Experiments on seven real-world datasets illustrate the effectiveness of MOGC.

*Keywords:* Graph clustering, Motifs, Higher-order structure, Spectral clustering, Optimization

---

## 1. Introduction

Nowadays, many complex interaction system can be naturally represented as graphs or networks, in which nodes refer to objects to be interested and edges representing the relationship among objects. Graph clustering which is one of the fundamental tasks in graph mining, aims to partition the graph into several densely connected groups with tight internal connections and sparse external connections. Graph clustering has been widely applied in many applications, such as social network, and computer vision.

Although many graph clustering methods have been proposed [1], most of them focus on the lower-order structure at the level of individual nodes and edges, and ignore the higher-order structure in the network. An important higher-order structure is network motif, which is defined as the building block of networks. Recently, some motif-based higher-order graph clustering methods [2][3][4] have been proposed, they often perform clustering on a motif-based hypergraph constructed by utilizing the co-occurrence information of two nodes in one motif instance. Motif characterizes higher-order network structures to provide new insights into the organization of complex systems beyond the clustering of nodes based on edges [4]. However, previous higher-order clustering methods assume that the motif-based hypergraph

is a connected graph, which is not hold in some real-world networks. The motif-based hypergraph usually become fragmented, in which the original connected graph may be fragmented into a large number of connected components and isolated nodes. Then in the process of clustering nodes, these isolated nodes will not be supported by original network, which makes the class label of isolated nodes present randomness. Only a few works [5][6] aim to address the challenges of hypergraph fragmentations, these works all focus on one kind of motif and utilize edges to solve the fragmentation issue.

However, a large real-world network often consists of many motifs with various functional roles, and different organizational patterns (clustering results) would be revealed with different types of motifs. For example, some 3-node motifs and 4-node motifs are found to play different functional roles in biological systems [4]. Moreover, a node is likely to involved in more than one type of network motif, and the importance of different types of motifs for a node varies from node to node in real world [7]. Therefore, different motifs and sample nodes potentially offer unique contribution to the graph clustering task. For example, in Fig. 1, blue nodes are closely connected with larger weights based on triangle motif, while another six nodes are isolated. Based on 4-node motif, red nodes are well connected with larger weights, while others are isolated from red nodes. It is obvious that triangle motif based hypergraph could provide more connectivity information for blue nodes, 4-node motif based hypergraphs are useful to identify the cluster of red nodes, different motifs contribute differently for each node in the identification of communities. It should be noted that these differences could be node specific. For example, the isolated node #11 becomes outlier in triangle motif based

hypergraph and 4-node motif based hypergraph, edge-based graph is more informative to the partition of node #11. For the convenience of description, original edge-based graph is regarded as a kind of motif-based hypergraph in this paper. Thus, in order to achieve accurate clustering result, a more effective approach is to establish a flexible framework in which a weight for each motif of each node can be assigned and adjusted adaptively in the clustering process.

To tackle the above mentioned problems, we propose a framework to integrate multiple higher-order structures (motifs) and lower-order structure with a independent weighting scaler assigned to each motif for each node. The formulated optimization model is composed of two parts, the first term exploits the underlying cluster structure from the integrated hypergraph by evaluating the contribution of each motif to each vertex. Another term is regularization term of motif weight to each vertex, such that irrelevant hypergraph would be removed in the clustering process. The proposed optimization problem can be solved by alternating scheme, it is decomposed into two subproblems which can be analytically solved respectively. Extensive experiments are conducted on seven datasets, comparison results with existing methods illustrate the effectiveness of the proposed method. The code of MOGC is released in the link<sup>1</sup>.

---

<sup>1</sup><https://github.com/SCUTFT-ML/MOGC>

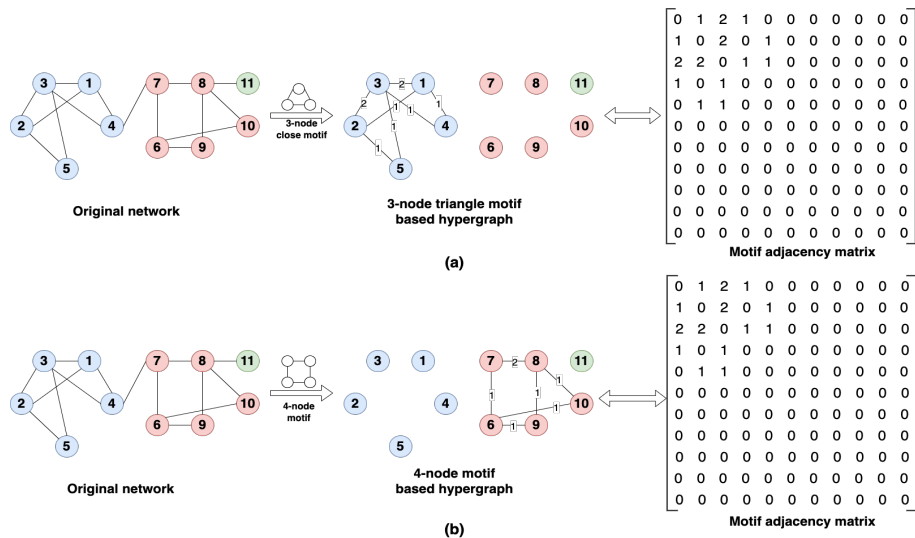


Figure 1: Illustration of fragmentation issue and different motifs' contributions to the graph clustering task: (a) Original network is fragmented into one connected component (blue nodes) and six isolated nodes (red nodes and green node) based on 3-node motif. (b) Original network is fragmented into one connected component (red nodes) and six isolated nodes (blue nodes and green node) based on 4-node motif. Original network contains edges with weight 1, numbers on edges demonstrate the edge weight in 3-node motif based hypergraph and 4-node motif based hypergraph, the corresponding motif adjacency matrix is shown in the third column.

## 2. Related Work

### 2.1. Lower-order Graph Clustering

Lower-order graph clustering finds the partition of vertices by utilizing the lower-order connectivity patterns of the graph at the level of nodes and edges. For undirected graph clustering, widely used methods concentrate on spectral clustering [1], random walk [8], matrix factorization [9], label propagation [10], affinity propagation [11], louvain method [12] and deep learning based methods [13]. For example, Nonnegative matrix factorization (NMF) [9] factorizes the node adjacency matrix into a basis matrix and an indicator matrix, indicator matrix is the data representation with clustering information. Affinity propagation [11] seeks cluster of nodes by similarities between pairs of nodes. The Louvain method [12] is a greedy optimization of

modularity, which measures the relative density of edges inside communities with respect to edges outside communities. Spectral clustering [1] utilizes the eigenvector of graph laplacian matrix to calculate the structure pattern, which is based on graph cut criteria, including ratio cut [14] and normalized cut [15]. Thus, the main focus of this paper is graph cut criteria based method.

Notation	Description
$\mathcal{G}; \mathcal{V}; \mathcal{E}$	Undirected graph; vertice set; edge set
$n; m; K$	The number of nodes; the number of motifs; the number of clusters
$\mathbf{A}; \mathbf{D}; \mathbf{L}$	Adjacency matrix; degree matrix; laplacian matrix of edge based graph
$\hat{\mathbf{B}}; p$	Adjacency matrix of bidirectional links; the number of nodes in motif
$\mathbf{B}; \mathcal{A}$	Binary matrix; the set of indices of the anchor nodes in motif.
$M_p^q, M_p^q(\mathbf{B}, \mathcal{A})$	Motif set
$\mathbf{A}_{M_p^q}; \mathbf{D}_{M_p^q}; \mathbf{L}_{M_p^q}$	Motif adjacency matrix; motif degree matrix; motif laplacian matrix.
$\mathbf{W}_{M_p^q}$	Indicator matrix of isolated nodes based on motif $M_p^q$ .
$\Lambda; \tilde{\Lambda}$	importance weight of motifs to nodes; the eigenvalue matrix
$\mathbf{A}_f$	Adjacency matrix with both higher-order and lower-order structures
$\mathbf{D}_f; \mathbf{L}_f$	Degree matrix; laplacian matrix of $\mathbf{A}_f$
$\theta_1, \theta_2; \alpha$	Lagragian multiplier parameters; trade-off parameter

Table 1: Summary of notations, different notations are separated by a semicolon (;).

## 2.2. Motif-based Graph Clustering

Many motif-based graph clustering methods have been proposed. For example, a generalized higher-order graph clustering [4] is proposed by extending conductance metric in traditional spectral graph theory to motif

conductance. Motif-modularity is proposed to define the class of nodes [16]. [3] develops triangle conductance and generalizes random walk to triangle based higher-order graph. [17] proposes motif-based approximated personalized PageRank algorithm to perform local graph clustering with higher-order structures. A graph sparsification method based on motif is designed to improve efficiency and quality of graph clustering [18]. A motif correlation clustering technique for overlapping community detection is developed by minimizing the number of clustering errors associated with both edges and motifs [19]. Edge based and motif based multiplex networks are constructed for community detection to reduce information loss during the aggregation of multiplex networks [20].

All the above motif-based graph clustering methods ignore the fragmentation issues resulting from motif-based hypergraph construction, which leads to clustering accuracy degradation. Several methods have been proposed to address this issue, a edge enhancement approach is proposed in [5] by injecting original graph edges into the high-order graph. A micro-unit modularity is designed by constructing a micro-unit connection network with integrating both lower-order structure and higher-order structure [21]. A hybrid-order stochastic block model is designed from the perspective of generative model [22]. Both an asymmetric triangle and edges are considered as clustering measurements to address fragmentation issue [23]. [24] introduces the definition of mixed-order cut criteria, based on it, spectral clustering is performed on the mixed-order adjacency matrix generated by random walks and graph laplacian. [25] firstly construct sub-higher order network and the corresponding sub-lower order network based on a kind of motif by eliminating

isolated nodes, then community detection is achieved by contrastive learning between above two networks. Finally, the isolated nodes are labelled by label propagation on edge-based graph.

However, current existing defragmentation methods mainly focus on integrating edges and one kind of motif with ignoring other useful motifs. Therefore, we propose a multi-order graph clustering model (MOGC) to integrate multiple motifs and edge information in order to resolve fragmentation issue and achieve more accurate partition results simultaneously.

### 3. Preliminaries

Given an undirected graph  $\mathcal{G} = \{\mathcal{V}, \mathcal{E}\}$ , where  $\mathcal{V} = \{v_1, \dots, v_n\}$  is a set of  $n$  vertices, and  $\mathcal{E}$  represents the set of edges among vertices. The corresponding adjacency matrix  $\mathbf{A} \in \mathbb{R}^{n \times n}$  denotes the similarity between each pair of nodes, in which  $\mathbf{A}_{i,j}$  is the similarity between vertice  $v_i$  and vertice  $v_j$ .  $\mathbf{A}_{i,j} = 0$  when there is no edge between vertice  $v_i$  and  $v_j$ . The degree of vertice  $v_i$  is defined as  $d_i = \sum_{j=1}^n \mathbf{A}_{i,j}$ , the degree matrix  $\mathbf{D}$  is a diagonal matrix with the degrees  $d_1, d_2, \dots, d_n$  on the main diagonal. The laplacian matrix  $\mathbf{L}$  is constructed as  $\mathbf{L} = \mathbf{D} - \mathbf{A}$ .

#### 3.1. Network Motif

The higher-order structure is characterized by motifs, according to [4], a network motif can be defined as:

**Definition 1. Network Motif.** A  $p$ -node motif  $M_p^q$  is defined by a tuple  $(\mathbf{B}, \mathcal{A})$ ,  $\mathbf{B}$  is a  $p \times p$  binary matrix and  $\mathcal{A} \subset \{1, 2, \dots, p\}$  is the set of indices of the anchor nodes.

Here  $\mathbf{B}$  encodes edge pattern between  $p$  nodes, and  $\mathcal{A}$  denotes a subset of the  $p$  nodes for defining the motif-based adjacency matrix. In other words, two nodes will be regarded as occurring in a given motif only when their indices belong to  $\mathcal{A}$ . When  $\mathcal{A}$  is the entire set of nodes, it is called simple motif, otherwise it is anchored motif. In this paper, we mainly focus on simple motif, a simple example for motif with 3 nodes is shown in Fig. 2.

**Definition 2. Motif Set.** *The motif set, denoted as  $M_p^q(\mathbf{B}, \mathcal{A})$ , is defined in an undirected graph  $\mathcal{G}$  as:*

$$M_p^q(\mathbf{B}, \mathcal{A}) = \{(set(\mathbf{v}), set(\chi_{\mathcal{A}}(\mathbf{v}))) | \mathbf{v} \in V^p, v_1, \dots, v_p, distinct, \mathbf{A}_{\mathbf{v}} = \mathbf{B}\}$$

where  $\mathbf{v}$  is an vector representing the indices of  $p$  nodes, and  $\chi_{\mathcal{A}}$  is a selection function taking the subset of a  $p$ -tuple indexed by  $\mathcal{A}$ , and  $set(\cdot)$  is the operator taking an ordered tuple to an unordered set, e.g.,  $set((v_1, v_2, \dots, v_p)) = \{v_1, v_2, \dots, v_p\}$ .  $\mathbf{A}_{\mathbf{v}}$  is the  $p \times p$  adjacency matrix on the subgraph induced by the  $p$  nodes of the ordered vector  $\mathbf{v}$ . Furthermore, any  $(set(\mathbf{v}), set(\chi_{\mathcal{A}}(\mathbf{v}))) \in M_p^q(\mathbf{B}, \mathcal{A})$  is a *motif instance*. In this paper, we will use  $M_p^q$  to represent  $M_p^q(\mathbf{B}, \mathcal{A})$  for simplicity.

### 3.2. Motif Adjacency matrix

**Definition 3. Motif Adjacency Matrix.** *Given a motif set  $M_p^q$ , its corresponding motif adjacency matrix is defined as  $(\mathbf{A}_{M_p^q})_{ij} = \sum_{(set(\mathbf{v}), set(\chi_{\mathcal{A}}(\mathbf{v})))} \mathbf{1}(i, j \subset set(\chi_{\mathcal{A}}(\mathbf{v})))$ , for  $i \neq j$ .  $\mathbf{1}(x)$  is a function, where  $\mathbf{1}(x)$  is 1 when  $x$  is true, otherwise it is 0.*

Note that  $(\mathbf{A}_{M_p^q})_{ij}$  denotes the number of motif instances when node  $v_i$  and  $v_j$  co-occur in the same  $p$ -node motif  $M_p^q$ . The larger  $(\mathbf{A}_{M_p^q})_{ij}$  is, the more

significant the relation between node  $v_i$  and  $v_j$  is within motif  $M_p^q$ . A concrete example of motif-based adjacency matrix is shown in Fig. 1. After the motif-based adjacency matrix is generated, the motif diagonal degree matrix is defined as  $(\mathbf{D}_{M_p^q})_{ii} = \sum_{j=1}^n (\mathbf{A}_{M_p^q})_{ij}$  and the motif Laplacian is  $\mathbf{L}_{M_p^q} = \mathbf{D}_{M_p^q} - \mathbf{A}_{M_p^q}$ .

Generally, the construction of  $\mathbf{A}_{M_p^q}$  is related to subgraph counting in large graphs [26][27][28]. We explore motifs with different sizes, including 3-node, 4-node and 5-node motifs in this paper.

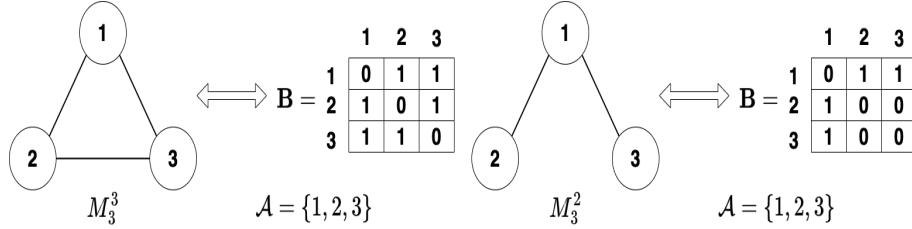


Figure 2: Network motif example for 3-node motifs.  $M_3^3$  and  $M_3^2$  are simple motifs, since the anchor set  $\mathcal{A}$  contains all of the nodes in  $M_3^3$  and  $M_3^2$ .  $\mathbf{B}$  is the binary matrix encoding edge pattern of corresponding motif.

### 3.2.1. 3-node Motif-based Adjacency Matrix Construction

For undirected graph  $\mathcal{G}$ , there are two different kinds of 3-node motifs shown in Fig. 2. Let  $\hat{\mathbf{B}}$  is the adjacency matrix of the bidirectional links of  $\mathcal{G}$ , then  $\hat{\mathbf{B}} = \mathbf{A} \circ \mathbf{A}^T$  according to [4], where  $\circ$  denotes the Hadamard product. For the motif  $M_3^3$ , the corresponding motif-based adjacency matrix  $\mathbf{A}_{M_3^3} = (\hat{\mathbf{B}} \cdot \hat{\mathbf{B}}) \circ \hat{\mathbf{B}}$ . It is very efficient to generate  $M_3^3$  motif-based adjacency matrix when the edge based adjacency matrix  $\mathbf{A}$  is sparse. For the motif  $M_3^2$ , we obtain the bidirectional links of  $\mathcal{G}$ , then enumerate all bidirectional links to generate  $M_3^2$  motif-based adjacency matrix  $\mathbf{A}_{M_3^2}$  according to [4].

### 3.2.2. 4-node and 5-node Motif-based Adjacency Matrix Construction

For a motif with  $p$  nodes,  $p = 4$  or  $p = 5$ , we need count all motif instances in the graph to calculate its corresponding motif-based adjacency matrix.  $\mathcal{O}(n^p)$  time is needed for enumerating all motif instances, the computation cost will increase dramatically with the increase of number of nodes. Moreover, there are too many isomorphic types of motifs. For example, there are 199 4-node motifs, 9364 5-node motifs [28]. Several methods with available softwares have been proposed to discover motif efficiently [26][27][28]. Hence, for the construction of  $p$ -node motif-based adjacency matrix, we firstly utilize a sampling method [28] with software mFinder<sup>1</sup> to detect motifs, which samples numerous  $p$ -node motifs based on the probability distribution derived from the frequency of various types of  $p$ -node motifs. Besides, mFinder also can generate all motif instances for each type of  $p$ -node motifs. Finally, we input all motif instances into Algorithm 1 in [29] to construct  $p$ -node motif-based adjacency matrix.

## 4. The Proposed Method

Given a graph  $\mathcal{G} = \{\mathcal{V}, \mathcal{E}\}$  and a motif  $M_p^q$ , we can obtain a symmetric and weighted motif adjacency matrix  $\mathbf{A}_{M_p^q} \in \mathbb{R}^{n \times n}$ . Note that motif  $M_p^q$  can be higher-order structure or lower-order structure, e.g., edge, 3-node motif, 4-node motif. In order to tackle the hypergraph fragmentation issue, we introduce a diagonal matrix  $\mathbf{W}_{M_p^q}$  to denote the isolated nodes based on motif  $M_p^q$ , if the  $i$ -th node is a isolated node in the corresponding higher-order

---

<sup>1</sup><https://www.weizmann.ac.il/mcb/UriAlon/download/network-motif-software>

graph, then  $(\mathbf{W}_{M_p^q})_{i,i} = 0$ , otherwise  $(\mathbf{W}_{M_p^q})_{i,i} = 1$ .

Moreover, assuming there are  $m$  different motifs  $M_{p_j}^{q_j}$  with  $j \in [1, m]$ , we introduce a nonnegative matrix  $\mathbf{\Lambda} \in \mathbb{R}^{n \times m}$  to denote the weight of each motif for each node. Each element  $\mathbf{\Lambda}_{i,j}$  ( $\forall i \in [1, n], j \in [1, m], \mathbf{\Lambda}_{i,j} \geq 0$ ) is the weight of motif  $M_{p_j}^{q_j}$  for node  $v_i$ , which illustrates the importance of motif  $M_{p_j}^{q_j}$  to node  $v_i$ . For example, in Fig. 1, the node #11 has connectivity with other nodes in edge-based graph, while it becomes outlier in 3-node motif based hypergraph and 4-node motif based hypergraph. Therefore, the importance of edge, 3-node motif, and 4-node motif for node #11 are different, and the weight of edge for node #11 should be highest. Note that if  $i$ -th node is a isolated node under motif  $M_{p_j}^{q_j}$ , then we set  $\mathbf{\Lambda}_{i,j} = 0$ . Therefore, to retain both higher-order structure and lower-order structure, we fuse the information from  $m$  motifs by  $\sum_{j=1}^m \mathbf{W}_{M_{p_j}^{q_j}} \mathbf{A}_{M_{p_j}^{q_j}} \mathit{diag}(\mathbf{\Lambda}_{:,j})$ . In order to guarantee symmetry of combined adjacent matrix, we set:

$$\mathbf{A}_f = \frac{1}{2} \sum_{j=1}^m (\mathbf{W}_{M_{p_j}^{q_j}} \mathbf{A}_{M_{p_j}^{q_j}} \mathit{diag}(\mathbf{\Lambda}_{:,j}) + \mathit{diag}(\mathbf{\Lambda}_{:,j}) \mathbf{A}_{M_{p_j}^{q_j}} \mathbf{W}_{M_{p_j}^{q_j}}) \quad (1)$$

Here,  $\mathit{diag}()$  converts a vector into an diagonal matrix with vector as the diagonal elements, and  $\mathbf{\Lambda}_{:,j}$  is the  $j$ -th column of  $\mathbf{\Lambda}$ , it denotes the importance weight of motif  $M_{p_j}^{q_j}$  for every node in the graph. After obtaining fused symmetric adjacency matrix  $\mathbf{A}_f$ , we can apply popular spectral clustering on fused adjacency matrix, it is formulated as:

$$\min_{\mathbf{\Lambda}, \mathbf{U}} \mathit{tr}(\mathbf{U}^T \mathbf{L}_f \mathbf{U}) \quad s.t. \quad \mathbf{U}^T \mathbf{D}_f \mathbf{U} = \mathbf{I} \quad (2)$$

Here  $\mathbf{L}_f = \mathbf{D}_f - \mathbf{A}_f$ ,  $\mathbf{D}_f$  is a diagonal degree matrix,  $\mathit{tr}()$  denotes the trace,  $\mathbf{U} \in \mathbb{R}^{n \times K}$  is the indicator matrix, which contains the clustering information.

Eq. (2) can avoid the degenerated case that all nodes are partitioned into one connected component [15]. The combined adjacent matrix  $\mathbf{A}_f$  depends on unknown variable  $\mathbf{\Lambda}$ , which denotes the importance weight of each motif for each node. To determine appropriate weights that mitigate the influence of irrelevant motifs while reinforcing meaningful ones, we constrain the sum of all motif weights for each node equal to one, i.e.,  $\sum_{j=1}^m \Lambda_{i,j} = 1, \forall i \in [1, n]$ . Finally, the multi-order graph clustering (MOGC) with adaptive weights learning mechanism is formulated as:

$$\min_{\mathbf{\Lambda}, \mathbf{U}} tr(\mathbf{U}^T \mathbf{L}_f \mathbf{U}) + \alpha \|\mathbf{\Lambda}\|_F^2, \quad s.t. \quad \mathbf{U}^T \mathbf{D}_f \mathbf{U} = \mathbf{I}, \quad \mathbf{\Lambda} \mathbf{1}_m = \mathbf{1}_n, \quad \mathbf{\Lambda} \geq 0 \quad (3)$$

$\mathbf{1}_m$  is a vector of length  $m$  with all the elements being 1,  $\mathbf{I}$  is the identity matrix, the second term  $\|\mathbf{\Lambda}\|_F^2$  forces a smooth solution, such that irrelevant hypergraphs would be removed in the clustering process.  $\alpha$  is a trade-off parameter.

## 5. Optimization

It is difficult to solve Eq. (3) directly, since both  $\mathbf{L}_f$  and  $\mathbf{D}_f$  depend on unknown variable  $\mathbf{\Lambda}$ . We use alternating optimization to solve Eq. (3).

### 5.1. Fix $\mathbf{\Lambda}$ , solve $\mathbf{U}$ :

When  $\mathbf{\Lambda}$  is fixed, the minimization problem Eq.(3) would become:

$$\min_{\mathbf{U}} tr(\mathbf{U}^T \mathbf{L}_f \mathbf{U}) \quad s.t. \quad \mathbf{U}^T \mathbf{D}_f \mathbf{U} = \mathbf{I}. \quad (4)$$

Since  $\mathbf{L}_f$  is symmetric, Eq. (4) is degenerated to the generalized eigenvalue problem [15] as follows:

$$\mathbf{L}_f \mathbf{U} = \mathbf{D}_f \mathbf{U} \tilde{\mathbf{\Lambda}} \quad (5)$$

where  $\tilde{\Lambda} = \text{diag}(\tilde{\lambda}_1, \tilde{\lambda}_2, \dots, \tilde{\lambda}_n)$  is the eigenvalue matrix, the solution of  $\mathbf{U}$  is given by the corresponding  $K$  eigenvectors corresponding to the first  $K$  smallest eigenvalues of generalized eigenvalue problem Eq. (5).

5.2. Fix  $\mathbf{U}$ , solve  $\Lambda$ :

When  $\mathbf{U}$  is fixed, the minimization problem Eq. (3) would become:

$$\min_{\Lambda} \text{tr}(\mathbf{U}^T \mathbf{L}_f \mathbf{U}) + \alpha \|\Lambda\|_F^2 \quad \text{s.t.} \quad \mathbf{U}^T \mathbf{D}_f \mathbf{U} = \mathbf{I}, \Lambda \mathbf{1}_m = \mathbf{1}_n, \Lambda \geq 0 \quad (6)$$

Let  $\mathbf{U}_k$  denotes the  $k$ -th column of  $\mathbf{U}$ . Because  $\mathbf{A}_f$  satisfies Eq. (1), and  $\mathbf{L}_f = \mathbf{D}_f - \mathbf{A}_f = \text{diag}(\mathbf{A}_f \mathbf{1}_n) - \mathbf{A}_f$ . Then Eq. (6) would become

$$\begin{aligned} \min_{\Lambda} \sum_{k=1}^K \mathbf{U}_k^T \text{diag}(\mathbf{A}_f \mathbf{1}_n) \mathbf{U}_k - \sum_{k=1}^K \mathbf{U}_k^T \mathbf{A}_f \mathbf{U}_k + \alpha \|\Lambda\|_F^2 \quad (7) \\ \text{s.t.} \quad \mathbf{U}_k^T \mathbf{D}_f \mathbf{U}_k = 1, \Lambda \mathbf{1}_m = \mathbf{1}_n, \Lambda \geq 0 \end{aligned}$$

Let  $\tilde{\mathbf{A}}_k = [\mathbf{U}_k^T \mathbf{W}_{M_{p_1}^{q_1}} \mathbf{A}_{M_{p_1}^{q_1}} \text{diag}(\mathbf{U}_k), \dots, \mathbf{U}_k^T \mathbf{W}_{M_{p_m}^{q_m}} \mathbf{A}_{M_{p_m}^{q_m}} \text{diag}(\mathbf{U}_k)]$ , and  $\tilde{\Lambda} = [\Lambda_{:,M_{p_1}^{q_1}}^T, \dots, \Lambda_{:,M_{p_m}^{q_m}}^T]^T$ , then

$$\begin{aligned} \sum_{k=1}^K \mathbf{U}_k^T \mathbf{A}_f \mathbf{U}_k &= \frac{1}{2} \sum_{k=1}^K \sum_{j=1}^m \mathbf{U}_k^T [\text{diag}(\Lambda_{:,M_{p_j}^{q_j}}) \mathbf{A}_{M_{p_j}^{q_j}} \mathbf{W}_{M_{p_j}^{q_j}} + \mathbf{W}_{M_{p_j}^{q_j}} \mathbf{A}_{M_{p_j}^{q_j}} \text{diag}(\Lambda_{:,M_{p_j}^{q_j}})] \mathbf{U}_k \\ &= \sum_{k=1}^K \sum_{j=1}^m \mathbf{U}_k^T \mathbf{W}_{M_{p_j}^{q_j}} \mathbf{A}_{M_{p_j}^{q_j}} \text{diag}(\mathbf{U}_k) \Lambda_{:,M_{p_j}^{q_j}} = \sum_{k=1}^K \tilde{\mathbf{A}}_k \tilde{\Lambda} \quad (8) \end{aligned}$$

Similarly, it is easy to derive that  $\text{diag}(\mathbf{A}_f \mathbf{1}_n) = \frac{1}{2} \sum_{j=1}^m \text{diag}(\Lambda_{:,M_{p_j}^{q_j}}) \text{diag}(\mathbf{A}_{M_{p_j}^{q_j}} \mathbf{W}_{M_{p_j}^{q_j}} \mathbf{1}_n) + \text{diag}(\mathbf{W}_{M_{p_j}^{q_j}} \mathbf{A}_{M_{p_j}^{q_j}} \text{diag}(\Lambda_{:,M_{p_j}^{q_j}}) \mathbf{1}_n)$ , then

$$\begin{aligned} \sum_{k=1}^K \mathbf{U}_k^T \text{diag}(\mathbf{A}_f \mathbf{1}_n) \mathbf{U}_k &= \frac{1}{2} \sum_{k=1}^K \sum_{j=1}^m \mathbf{U}_k^T \text{diag}(\mathbf{A}_{M_{p_j}^{q_j}} \mathbf{W}_{M_{p_j}^{q_j}} \mathbf{1}_n) \text{diag}(\mathbf{U}_k) \Lambda_{:,M_{p_j}^{q_j}} \\ &\quad + \mathbf{U}_k^T \text{diag}(\mathbf{U}_k) \mathbf{W}_{M_{p_j}^{q_j}} \mathbf{A}_{M_{p_j}^{q_j}} \text{diag}(\mathbf{1}_n) \Lambda_{:,M_{p_j}^{q_j}} \quad (9) \end{aligned}$$

Let  $\hat{\mathbf{A}}_k = [\mathbf{U}_k^T \text{diag}(\mathbf{A}_{M_{p_1}^{q_1}} \mathbf{W}_{M_{p_1}^{q_1}} \mathbf{1}_n) \text{diag}(\mathbf{U}_k), \dots, \mathbf{U}_k^T \text{diag}(\mathbf{A}_{M_{p_m}^{q_m}} \mathbf{W}_{M_{p_m}^{q_m}} \mathbf{1}_n) \text{diag}(\mathbf{U}_k)]$ ,  
 $\bar{\mathbf{A}}_k = [\mathbf{U}_k^T \text{diag}(\mathbf{U}_k) \mathbf{W}_{M_{p_1}^{q_1}} \mathbf{A}_{M_{p_1}^{q_1}}, \dots, \mathbf{U}_k^T \text{diag}(\mathbf{U}_k) \mathbf{W}_{M_{p_m}^{q_m}} \mathbf{A}_{M_{p_m}^{q_m}}]$ , then

$$\sum_{k=1}^K \mathbf{U}_k^T \text{diag}(\mathbf{A}_f \mathbf{1}_N) \mathbf{U}_k = \frac{1}{2} \sum_{k=1}^K (\hat{\mathbf{A}}_k + \bar{\mathbf{A}}_k) \tilde{\mathbf{\Lambda}}$$

Finally, according to Eq. (8) and Eq. (9), the optimization problem Eq. (7) can be solved instead of

$$\min_{\tilde{\mathbf{\Lambda}}} \mathbf{V} \tilde{\mathbf{\Lambda}} + \alpha \|\tilde{\mathbf{\Lambda}}\|_F^2 \quad s.t. \quad (\hat{\mathbf{A}}_k + \bar{\mathbf{A}}_k) \tilde{\mathbf{\Lambda}} = \mathbf{1}, \mathbf{M} \tilde{\mathbf{\Lambda}} = \mathbf{1}_n, \tilde{\mathbf{\Lambda}} \geq 0, \forall k \in [1, K] \quad (10)$$

Here  $\mathbf{V} = \frac{1}{2} \sum_{i=1}^K (\hat{\mathbf{A}}_i + \bar{\mathbf{A}}_i) - \sum_{i=1}^K \tilde{\mathbf{A}}_i$  with  $\mathbf{V} \in \mathbb{R}^{1 \times nm}$ , and  $\mathbf{M} = [\mathbf{I}_n, \dots, \mathbf{I}_n]$  with  $\mathbf{M} \in \mathbb{R}^{n \times nm}$ . Let  $\mathbf{P} = [(\hat{\mathbf{A}}_1 + \bar{\mathbf{A}}_1)^T, (\hat{\mathbf{A}}_2 + \bar{\mathbf{A}}_2)^T, \dots, (\hat{\mathbf{A}}_K + \bar{\mathbf{A}}_K)^T]^T$ . Then for Eq. (10), it becomes

$$\min_{\tilde{\mathbf{\Lambda}}} \mathbf{V} \tilde{\mathbf{\Lambda}} + \alpha \|\tilde{\mathbf{\Lambda}}\|_F^2 \quad s.t. \quad \mathbf{P} \tilde{\mathbf{\Lambda}} = \mathbf{1}_K, \mathbf{M} \tilde{\mathbf{\Lambda}} = \mathbf{1}_n, \tilde{\mathbf{\Lambda}} \geq 0 \quad (11)$$

Denote  $\Phi_1 \in \mathbb{R}^{n \times 1}$ ,  $\Phi_2 \in \mathbb{R}^{K \times 1}$  as the Lagrangian multiplier, then we can write the Lagrangian function of Eq. (11) as

$$\mathbb{F} = \mathbf{V} \tilde{\mathbf{\Lambda}} + \alpha \|\tilde{\mathbf{\Lambda}}\|_F^2 - \Phi_1^T (\mathbf{M} \tilde{\mathbf{\Lambda}} - \mathbf{1}_n) - \Phi_2^T (\mathbf{P} \tilde{\mathbf{\Lambda}} - \mathbf{1}_K) - \xi_+(\tilde{\mathbf{\Lambda}}) \quad (12)$$

$\xi_+$  represents the delta function which provides  $+\infty$  to the negative value.

The derivative of Eq. (12) with respect to  $\tilde{\mathbf{\Lambda}}$  is

$$\frac{\partial \mathbb{F}}{\partial \tilde{\mathbf{\Lambda}}} = 2\alpha \tilde{\mathbf{\Lambda}} + \mathbf{V}^T - \mathbf{M}^T \Phi_1 - \mathbf{P}^T \Phi_2 \quad (13)$$

With KKT condition, the optimal solution can be defined as

$$\tilde{\mathbf{\Lambda}} = Proj\left(\frac{\mathbf{M}^T \Phi_1 + \mathbf{P}^T \Phi_2 - \mathbf{V}^T}{2\alpha}\right)_+ \quad (14)$$

Where  $Proj(\tilde{\Lambda})_+$  indicates that if  $\tilde{\Lambda} < 0$ , then set  $\tilde{\Lambda} = 0$ . Since  $\mathbf{M}\tilde{\Lambda} = \mathbf{1}_n, \mathbf{P}\tilde{\Lambda} = \mathbf{1}_K$ , then it is easy to derive that the optimal  $\Phi_1$  and  $\Phi_2$  are

$$\begin{aligned}\Phi_1 &= [\mathbf{M}\mathbf{M}^T - \mathbf{M}\mathbf{P}^T(\mathbf{P}\mathbf{P}^T)^{-1}\mathbf{P}\mathbf{M}^T]^{-1}[2\alpha\mathbf{1}_n + \mathbf{M}\mathbf{V}^T - \mathbf{M}\mathbf{P}^T(\mathbf{P}\mathbf{P}^T)^{-1}(2\alpha\mathbf{1}_K + \mathbf{P}\mathbf{V}^T)] \\ \Phi_2 &= [\mathbf{P}\mathbf{P}^T - \mathbf{P}\mathbf{M}^T(\mathbf{M}\mathbf{M}^T)^{-1}\mathbf{M}\mathbf{P}^T]^{-1}[2\alpha\mathbf{1}_K + \mathbf{P}\mathbf{V}^T - \mathbf{P}\mathbf{M}^T(\mathbf{M}\mathbf{M}^T)^{-1}(2\alpha\mathbf{1}_n + \mathbf{M}\mathbf{V}^T)]\end{aligned}\tag{15}$$

Actually the optimal  $\Phi_1$  and  $\Phi_2$  can be obtained by conjugate gradient method [30], the final solution of  $\tilde{\Lambda}$  can be obtained by Eq. (14) with Eq. (15), the solution of  $\Lambda$  can be obtained by reshaping vector  $\tilde{\Lambda}$  back to matrix.

Based on the above analysis, the detail process for solution Eq. (3) is shown in the Algorithm 1. Besides, the flowchart of our proposed methods is shown in Fig. (3).

---

**Algorithm 1** MOGC: Alternating method for solving Eq. (3)

---

**Input:** Given input  $\mathbf{A}_{M_{P_j}^{a_j}}, \mathbf{W}_{M_{P_j}^{a_j}}$ , the parameters  $\alpha, K$  and the stopping criterion  $\epsilon = 10^{-5}$ .

**Output:**  $\mathbf{U}$  and  $\Lambda$

- 1: **repeat**
  - 2:   Compute  $\mathbf{U}^k$  by (4).
  - 3:   Compute  $\tilde{\Lambda}$  by Eq. (14), and reshape  $\tilde{\Lambda}$  into  $n \times n$  matrix  $\Lambda$ .
  - 4: **until**  $\max\{\|\mathbf{U}^{k+1} - \mathbf{U}^k\|_F^2, \|\Lambda^{k+1} - \Lambda^k\|_F^2\} \leq \epsilon$ .
-

## 6. Theoretical Analysis

### 6.1. Convergence Analysis

Denote  $\mathcal{F} := \{(\mathbf{\Lambda}, \mathbf{U}) | \mathbf{U}^T \mathbf{D}_f \mathbf{U} = \mathbf{I}, \mathbf{\Lambda} \mathbf{1}_m = \mathbf{1}_n, \mathbf{\Lambda}_{i,j} \geq 0, (i, j) \in [1, n] \times [1, m]\}$

The minimization problem can be written as:

$$\min_{(\mathbf{\Lambda}, \mathbf{U}) \in \mathcal{F}} f(\mathbf{\Lambda}, \mathbf{U}), \text{ where } f(\mathbf{\Lambda}, \mathbf{U}) = \text{tr}(\mathbf{U}^T \mathbf{L}_f \mathbf{U}) + \alpha \|\mathbf{\Lambda}\|_F^2.$$

Let  $\{\mathbf{\Lambda}^{(k)}, \mathbf{U}^{(k)}\}_{k=0}^{+\infty}$  be the iterative sequence generated by the alternating minimization.

**Definition 4.** *The values of objective function  $f$  along the iterative sequence  $\{\mathbf{\Lambda}^{(k)}, \mathbf{U}^{(k)}\}_{k=0}^{+\infty}$  is monotonically decreasing and converge to a finite value  $\check{f} \geq 0$ , i.e.,  $0 \leq \lim_{k \rightarrow +\infty} f(\mathbf{\Lambda}^{(k)}, \mathbf{U}^{(k)}) = \check{f} < +\infty$  and  $\check{f} = \inf_{k \geq 0} f(\mathbf{\Lambda}^{(k)}, \mathbf{U}^{(k)})$ .*

**proof 1.** *The alternating iterative process implies that*

$$f(\mathbf{\Lambda}^{(k)}, \mathbf{U}^{(k)}) \geq f(\mathbf{\Lambda}^{(k)}, \mathbf{U}^{(k+1)}) \geq f(\mathbf{\Lambda}^{(k+1)}, \mathbf{U}^{(k+1)}),$$

*which means the sequence  $\{f(\mathbf{\Lambda}^{(k)}, \mathbf{U}^{(k)})\}_{k=1}^{+\infty}$  is monotonically decreasing. Moreover, it is clear that  $\{\mathbf{\Lambda}^{(k)}, \mathbf{U}^{(k)}\}_{k=0}^{+\infty} \subset \mathcal{F}$ . Therefore,  $+\infty > f(\mathbf{\Lambda}^{(k)}, \mathbf{U}^{(k)}) \geq 0$ . Hence,  $\{f(\mathbf{\Lambda}^{(k)}, \mathbf{U}^{(k)})\}_{k=1}^{+\infty}$  is a monotonically decreasing upper and lower bounded sequence. Hence, there exists a finite constant  $\check{f} \in [0, +\infty)$  such that  $\lim_{k \rightarrow +\infty} f(\mathbf{\Lambda}^{(k)}, \mathbf{U}^{(k)}) = \check{f}$ . The monotonicity of  $\{f(\mathbf{\Lambda}^{(k)}, \mathbf{U}^{(k)})\}_{k=1}^{+\infty}$  implies that  $\check{f} = \inf_{k \geq 0} f(\mathbf{\Lambda}^{(k)}, \mathbf{U}^{(k)})$ . The proof is complete.*

### 6.2. Computational Complexity

We analyze the complexity of the proposed MOSC method as follows. In general, the complexity of this algorithm is governed by the computation of motif adjacency matrix and the alternating minimization algorithm in Algorithm. 1.

For sparse real networks with adjacency matrix  $\mathbf{A}$ , the symmetric matrix  $\mathbf{A}$  has  $|\mathbf{A}|$  non-zero elements, we assume that there is  $|\mathbf{A}_i|$  non-zero elements at the  $i$ -th column. According to the introduction of section 3.2.1, for the motif  $M_3^3$ , its corresponding motif based adjacency matrix construction is  $\mathbf{A}_{M_{p_j}^{q_j}} = (\mathbf{A} \circ \mathbf{A}^T) \cdot (\mathbf{A} \circ \mathbf{A}^T) \circ (\mathbf{A} \circ \mathbf{A}^T)$ , where  $\mathbf{A} \circ \mathbf{A}^T$  takes  $|\mathbf{A}|$  flops, and the  $\cdot$  operation takes  $\sum_{i=1}^n |\mathbf{A}_i|^2$  flops, so the total flops of  $M_3^3$  motif based adjacency matrix construction is  $\sum_{i=1}^n |\mathbf{A}_i|^2 + 3|\mathbf{A}|$  and the corresponding computational complexity is  $O(\sum_{i=1}^n |\mathbf{A}_i|^2)$ .  $M_3^2$  based adjacency matrix is generated according to [4],  $O(\frac{nJ_i}{2})$  complexity is required, where  $J_i$  is the non-zero elements at the  $i$ -th row of bidirection subgraph adjacency matrix  $\hat{\mathbf{B}}$  corresponding to  $\mathbf{A}$ .

For  $p$ -node motif with  $p = 4$  or  $p = 5$ , according to section 3.2.2, a sampling method with mFinder software is firstly applied to count all motif instances, which has total computation complexity of  $O(sp^{p+1})$ , where  $s$  is the number of samples [28]. Then, Algorithm 1 in [29] is executed to generate motif-based adjacent matrix, it has complexity  $O(s_p p^2)$ , where  $s_p$  denotes the number of generated motif instances of  $p$ -node motif. Therefore, the total complexity for calculating 4-node or 5-node based adjacent matrix is  $O(sp^{p+1} + s_p p^2)$ .

Next, we discuss the operation cost of the alternating minimization iterative process when the matrices  $\mathbf{A}_{M_{p_j}^{q_j}}$ ,  $\mathbf{W}_{M_{p_j}^{q_j}}$  are given. For the process of solving  $\mathbf{\Lambda}$  with fixed  $\mathbf{U}$ , the  $\mathbf{\Lambda}$  is calculated by Eq. (14), which requires the value of  $\Phi_1$ ,  $\Phi_2$ ,  $\mathbf{P}$  and  $\mathbf{V}$ . By definition of  $\Phi_1$  in Eq. (15), its evaluation requires  $(2K^2 + 5K + 1)mn + (4K^2 + 2K + 11)n + K^3 + K^2 + K$  flops using conjugate gradient solver. By definition of  $\Phi_2$  in Eq. (15), its evaluation requires  $(2K^2 + 3K + 2)mn + (2K^2 - K + 1)n + K^3/3 + 5K^2/2 + K/6$  flops. Besides, both of  $\mathbf{P}$  and  $\mathbf{V}$  depends on  $\tilde{\mathbf{A}}_i$ ,  $\hat{\mathbf{A}}_i$  and  $\bar{\mathbf{A}}_i$  for  $i = 1, 2, \dots, K$ . By definition of  $\tilde{\mathbf{A}}_i$ , its evaluation requires  $(2n - 1)m + 2\tilde{s}$  flops for each  $i$ . Here,  $\tilde{s}$  represents the total number of non-zero entries in  $\mathbf{A}_{M_{p_1}^{q_1}}, \dots, \mathbf{A}_{M_{p_m}^{q_m}}$ . By the definition of  $\hat{\mathbf{A}}_i$ , its evaluation requires  $2\tilde{s} + n$

flops for each  $i$ . By definition of  $\bar{\mathbf{A}}_i$ , its evaluation requires  $2\tilde{s}$  flops for each  $i$ . By definition of  $\mathbf{P}$ , its evaluation requires  $Kmn$  flops with the knowledge of  $\hat{\mathbf{A}}_i$  and  $\bar{\mathbf{A}}_i$ . By definition of  $\mathbf{V}$ , its evaluation requires  $2Kmn$  flops with the knowledge of  $\hat{\mathbf{A}}_i$ ,  $\bar{\mathbf{A}}_i$  and  $\tilde{\mathbf{A}}_i$ . Eq. (14) indicates that the evaluation of  $\mathbf{\Lambda}$  requires  $(2K + 2)mn$  flops with the knowledge of  $\Phi_1$ ,  $\Phi_2$  and  $\mathbf{V}$ . Therefore, the updating  $\mathbf{\Lambda}$  for fixed  $\mathbf{U}$  requires  $(4K^2 + 15K + 5)mn + (6K^2 + 3K + 12)n + (6\tilde{s} - m)K + 4K^3/3 + 7K^2/2 + 7K/6$  flops in total, and it is an  $O(K^2mn)$  sub-problem.

Now, let's focus on the process of updating  $\mathbf{U}$  with fixed  $\mathbf{\Lambda}$ . It is an eigenproblem for find the  $K$  eigenvectors corresponding to the  $K$  smallest eigenvalues of the symmetric matrix  $\mathbf{D}^{-\frac{1}{2}}\mathbf{L}\mathbf{D}^{-\frac{1}{2}}$ , which requires  $\mathcal{O}(K^2n)$  operations by the truncated SVD algorithm.

To conclude, each alternating minimization iteration requires  $\mathcal{O}(K^2mn)$  operations in total.

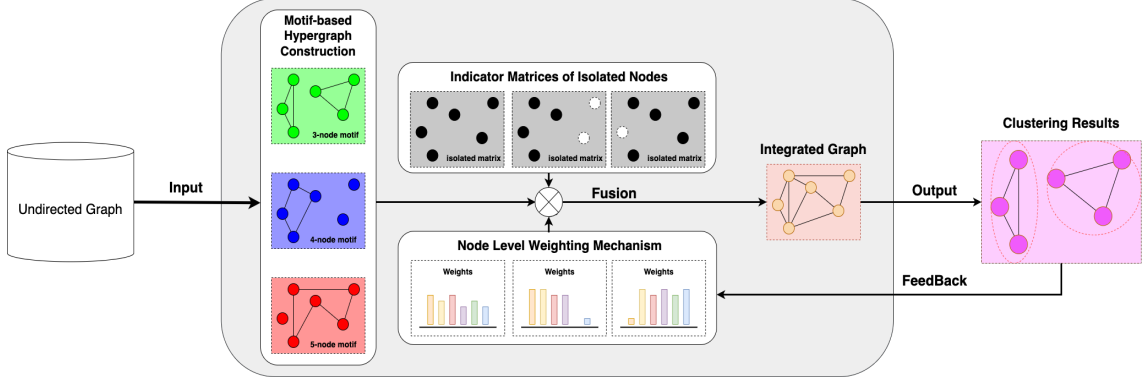


Figure 3: The flowchart of MOGC

## 7. Experiments

### 7.1. Testing Datasets

In this section, we conduct experiments on seven real datasets. **football**<sup>1</sup> contains 115 nodes connected with 616 edges which are partitioned into 12 groups. **polbooks**<sup>1</sup> is a network of 105 books with 441 edges, edges represent frequent copurchasing of books by the same buyers. Books belongs to 3 clusters. **polblogs**<sup>1</sup> is a network with 1490 weblogs (nodes) partitioned into 2 clusters and 19090 edges. **Cora**<sup>2</sup> consists of 2708 scientific publications classified into one of seven classes, nodes are connected with 5429 links. **email-Eu-core**<sup>3</sup> describes the email sent between members (nodes) within a large European research institution. The network contains 1005 nodes with 25571 edges are classified into one of 42 classes. **CiteSeer**<sup>2</sup> consists of 3312 scientific publications classified into one of six classes. It has 4732 links. **Pubmed**<sup>2</sup> consists of 19717 scientific publications with 44338 links classified into one of three classes. All datasets are undirected graph and self-loops are removed, the summary of them is shown in Table. 2.

Table 2: Summary of real datasets

Dataset	football	polbooks	polblogs	Cora	email-Eu-core	Citeseer	Pubmed
Nodes	115	105	1490	2708	1005	3312	19717
Edges	616	441	19090	5429	25571	4732	44324
Class	12	3	2	7	42	6	3

<sup>1</sup><http://www-personal.umich.edu/~mejn/netdata/>

<sup>2</sup><https://linqs.org/datasets/>

<sup>3</sup><https://snap.stanford.edu/data/email-Eu-core.html>

## 7.2. Comparison Methods

We mainly compare our method with several lower-order clustering methods and higher-order clustering methods. The lower-order clustering methods: **Spectral Clustering (SC)** [31] is performed on edge-based adjacency matrix. **Normalized Cut (Ncut)** [15] partitions graphs based on graph normalized cut. **Non-negative Matrix Factorization** [32] is performed on the graph adjacency matrix to obtain the group partition. **Affinity Propagation (AP)** [11] seeks clusters of nodes by similarities between pairs of nodes. **Node2vec+Kmeans (N2VKM)** [33] learns low-dimensional representations for vertices by biased random walk and skip-Gram, then K-means is performed to cluster the embedded vectors of vertices into several groups. The higher-order clustering methods include Motif\_SC [4], EdMot\_SC [5], MWLP [6], MOSC [24], CDMA [20] and MotifCC [25]. They can only utilize one kind of motif, while our method integrates information from multiple motifs. In the experiment, higher-order clustering methods with motif  $\mathbf{M}_q^p$  means motif  $\mathbf{M}_q^p$  is used to generate motif hypergraph. **Motif\_SC** [4] extends traditional spectral clustering to higher-order structure by constructing motif-based adjacency matrix. **EdMot\_SC** [5] proposes an edge enhancement approach to overcome hypergraph fragmentation issues by adding edges to generate hypergraph, then the new constructed adjacency matrix is used as input of spectral clustering to obtain final. **MWLP** [6] proposes motif-aware weighted label propagation method to integrate higher-order structure and original lower-order structure by reweighted network. **MOSC** [24] performs spectral clustering on the mixed-order adjacency matrix generated based on edge and one kind of motif by graph Laplacian. **CDMA** [20] proposes a multiplex network community detection algorithm based on edge and motif, only one layer is considered in order to make comparison with our method. **MotifCC** [25] performs deep contrastive learning on sub-higher order graph and sub-lower order graph, which generated from motif based graph

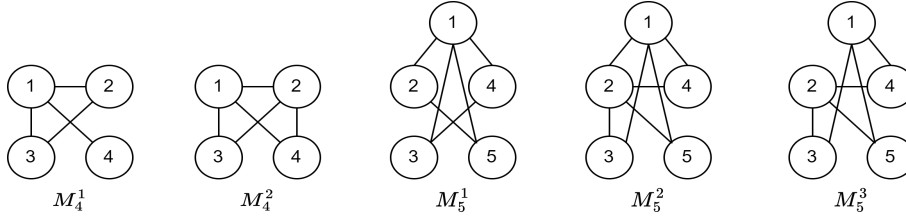


Figure 4: 4-node motif and 5-node motif used in the experiments.

and edge based graph separately.

### 7.3. Experiments Setting and Evaluation Measurements

For MOGC,  $\alpha$  is tuned in  $\{0.1, 0.2, \dots, 3\}$  and  $\{4, 5, \dots, 20\}$ , and then it is determined when best score is achieved. In addition, the walk length, the number of walks per node, the embedding dimension and the window size in Node2vec are set as 80, 10, 128, and 10 separately. Moreover, the hyperparameter  $p$  and in-out parameter  $q$  are tuned such that best performance is achieved. Best parameters reported in other comparison methods are used in the experiment. We set the number of clusters as the ground-truth communities for all methods.

We evaluate the clustering results using metrics like Rand Index (RI) [34] and Normalized Mutual Information (NMI) [35]. For all measurements, a higher value indicates better performance. All experiments are repeated for 20 times, the average metrics and their standard deviations are reported.

### 7.4. Experimental Results

#### 7.4.1. Results of 3-node Motifs

We firstly test our method on 3-node motif, there are 2 different types of 3-node motif for undirected graph, i.e.,  $M_3^3$  and  $M_3^2$  shown in Fig. 4. Then, we construct motif  $M_3^3$  and  $M_3^2$  based adjacency matrix introduced in section 3. The lower-order clustering methods including SC, Ncut, NMF, AP, N2VKM are tested on edge-based graph, the higher-order clustering methods utilizing one kind of motif and edge, including Motif\_SC, EdMot\_SC, MWLP, MOSC, CDMA, and MotifCC, are tested on edge-based graph and motif-based hypergraph. Our method MOGC can utilize lower-order graph and multiple higher-order hypergraphs, the results of MOGC with  $M_3^3$  and  $M_3^2$  on seven datasets mean that edge-based graph, motif  $M_3^3$

and motif  $M_3^2$  based hypergraphs are used in Algorithm 1. The experiment results for all methods on seven datasets are shown in Table. 3 and Table. 4, it shows that MOGC outperforms other methods with different motifs, which demonstrates the effectiveness of our method.

We further give a detailed analysis about the results. Firstly, Compared with traditional edge-based graph partition methods, the corresponding higher-order methods generally have higher accuracy than most of them, which illustrates that the higher-order structures play an important role in community discovery. Secondly, when motif  $M_3^3$  is adopted, MOGC has better performances than other higher-order graph clustering methods on almost all datasets. For Cora, Citeseer and Pubmed datasets with very sparse connectivity pattern, the accuracy of higher-order method Motif\_SC decreases greatly compared with edge-based method (SC), since Motif\_SC suffers from serious fragmentation issue. However, in terms of Rand Index, MOGC achieves about 70%, 65%, 65% improvements over Motif\_SC. This shows the effectiveness of MOGC in addressing the hypergraph fragmentation issue. Moreover, the accuracy of CDMA decreases significantly for Cora and Citeseer datasets with  $M_3^3$ , due to the ignorance of fragmentation issue in CDMA. Compared with state-of-the-art defragmented higher-order graph clustering methods (EdMot\_SC and MWLP), we also have much higher accuracy than others, which validates adaptive weights learning mechanism is more helpful than edge enhancement approaches in addressing hypergraph fragmentation issue. Compared with MOSC which combines edge and triangle adjacency matrices with mixing parameter, MOGC performs better on all datasets, it proves that more accurate results would be achieved by assigning weighting scaler to each motif for each node. Our method show better performances than MotifCC on almost all datasets, since MotifCC adopts two steps for community detection, label of all nonisolated nodes are obtained firstly by applying contrastive learning on

Table 3: Rand Index Results on seven real datasets (mean $\pm$ std).

	dataset	football	polbooks	polblogs	Cora	email-Eu-core	Citeseer	Pubmed
edge	SC	0.8967 $\pm$ 0.0000	0.6445 $\pm$ 0.0521	0.0005 $\pm$ 0.0000	0.2385 $\pm$ 0.0000	0.4145 $\pm$ 0.0188	0.3431 $\pm$ 0.0000	0.1123 $\pm$ 0.0000
	Ncut	0.0086 $\pm$ 0.0052	0.3524 $\pm$ 0.0782	0.3497 $\pm$ 0.0441	0.0027 $\pm$ 0.0016	0.0260 $\pm$ 0.0050	0.0638 $\pm$ 0.0145	0.0004 $\pm$ 0.0008
	NMF	0.8810 $\pm$ 0.0254	0.5679 $\pm$ 0.0523	0.8013 $\pm$ 0.0000	0.2745 $\pm$ 0.0209	0.4574 $\pm$ 0.0200	0.1584 $\pm$ 0.0108	0.0976 $\pm$ 0.0039
	AP	0.3426 $\pm$ 0.0460	0.1139 $\pm$ 0.0171	0.0501 $\pm$ 0.0021	0.0160 $\pm$ 0.0011	0.0739 $\pm$ 0.0067	0.0117 $\pm$ 0.0015	0.0011 $\pm$ 0.0002
	N2VKM	0.9836 $\pm$ 0.0000	0.8485 $\pm$ 0.0000	0.8186 $\pm$ 0.0000	0.8241 $\pm$ 0.0000	0.9553 $\pm$ 0.0000	0.7182 $\pm$ 0.0005	0.6905 $\pm$ 0.0000
$M_3^3$	Motif_SC	0.8967 $\pm$ 0.0273	0.6572 $\pm$ 0.0713	0.0036 $\pm$ 0.0000	0.0788 $\pm$ 0.0000	0.3243 $\pm$ 0.0104	0.0369 $\pm$ 0.0000	0.3511 $\pm$ 0.0078
	EdMot_SC	0.8967 $\pm$ 0.0000	0.6622 $\pm$ 0.0236	0.7956 $\pm$ 0.0000	0.3434 $\pm$ 0.0050	0.3667 $\pm$ 0.0119	0.1545 $\pm$ 0.0342	0.2623 $\pm$ 0.0000
	MWLP	0.9420 $\pm$ 0.0010	0.6689 $\pm$ 0.0138	0.5277 $\pm$ 0.0018	0.7761 $\pm$ 0.0024	0.1902 $\pm$ 0.0000	0.7813 $\pm$ 0.0004	0.6405 $\pm$ 0.0011
	MOSC	0.7733 $\pm$ 0.0596	0.6613 $\pm$ 0.0073	0.0004 $\pm$ 0.0000	0.0053 $\pm$ 0.0000	0.4718 $\pm$ 0.0211	0.3225 $\pm$ 0.0224	0.1880 $\pm$ 0.0762
	CDMA	0.9597 $\pm$ 0.0000	0.4844 $\pm$ 0.0000	0.5195 $\pm$ 0.0000	0.1999 $\pm$ 0.0000	0.7859 $\pm$ 0.0000	0.2169 $\pm$ 0.0000	0.3580 $\pm$ 0.0000
	MotifCC	0.9706 $\pm$ 0.0063	0.6774 $\pm$ 0.0563	0.7131 $\pm$ 0.0562	0.7334 $\pm$ 0.0015	0.9409 $\pm$ 0.0035	0.7147 $\pm$ 0.0006	0.5479 $\pm$ 0.0003
	MOGC	0.9830 $\pm$ 0.0047	0.8464 $\pm$ 0.0035	0.8963 $\pm$ 0.0000	0.7375 $\pm$ 0.0000	0.9564 $\pm$ 0.0102	0.6965 $\pm$ 0.0000	<b>0.6510</b> $\pm$ 0.0081
$M_3^2$	Motif_SC	0.8609 $\pm$ 0.0751	0.6636 $\pm$ 0.0451	0.8190 $\pm$ 0.0000	0.2726 $\pm$ 0.0000	0.4431 $\pm$ 0.0125	0.3461 $\pm$ 0.0000	0.2597 $\pm$ 0.0000
	EdMot_SC	0.8590 $\pm$ 0.0000	0.6667 $\pm$ 0.0080	0.8072 $\pm$ 0.0000	0.2726 $\pm$ 0.0000	0.4414 $\pm$ 0.0067	0.3461 $\pm$ 0.0000	0.2597 $\pm$ 0.0000
	MWLP	0.8900 $\pm$ 0.0015	0.6559 $\pm$ 0.0007	0.5847 $\pm$ 0.0000	0.7793 $\pm$ 0.0006	0.1485 $\pm$ 0.0000	0.7468 $\pm$ 0.0000	0.6405 $\pm$ 0.0013
	MOSC	0.7376 $\pm$ 0.0724	0.6326 $\pm$ 0.0070	0.8190 $\pm$ 0.0000	0.0055 $\pm$ 0.0000	0.4399 $\pm$ 0.0233	0.3212 $\pm$ 0.0214	0.2376 $\pm$ 0.0495
	CDMA	0.9408 $\pm$ 0.0000	0.7170 $\pm$ 0.0000	0.4996 $\pm$ 0.0000	0.4522 $\pm$ 0.0000	0.8306 $\pm$ 0.0000	0.3903 $\pm$ 0.0000	0.3995 $\pm$ 0.0000
	MotifCC	0.9617 $\pm$ 0.0090	0.7807 $\pm$ 0.0390	0.6838 $\pm$ 0.0435	0.7351 $\pm$ 0.0016	0.9355 $\pm$ 0.0032	0.7155 $\pm$ 0.0006	0.5454 $\pm$ 0.0002
	MOGC	<b>0.9858</b> $\pm$ 0.0108	<b>0.8555</b> $\pm$ 0.0000	<b>0.9110</b> $\pm$ 0.0000	0.7888 $\pm$ 0.0000	0.9608 $\pm$ 0.0009	0.7883 $\pm$ 0.0000	0.5405 $\pm$ 0.0015
$M_4^*$	Motif_SC	0.8242 $\pm$ 0.0000	0.6570 $\pm$ 0.0000	0.0509 $\pm$ 0.0000	0.1777 $\pm$ 0.0000	0.3858 $\pm$ 0.0000	0.0408 $\pm$ 0.0000	0.0007 $\pm$ 0.0000
	EdMot_SC	0.8242 $\pm$ 0.0000	0.6886 $\pm$ 0.0000	0.1628 $\pm$ 0.0818	0.3453 $\pm$ 0.0082	0.3933 $\pm$ 0.0036	0.1211 $\pm$ 0.0425	0.0626 $\pm$ 0.0003
	MWLP	0.9396 $\pm$ 0.0009	0.8209 $\pm$ 0.0141	0.5083 $\pm$ 0.0010	0.8024 $\pm$ 0.0005	0.9164 $\pm$ 0.0001	<b>0.8222</b> $\pm$ 0.0000	0.6400 $\pm$ 0.0000
	MOSC	0.7526 $\pm$ 0.0472	0.6484 $\pm$ 0.0086	0.7371 $\pm$ 0.2458	0.0544 $\pm$ 0.0028	0.3838 $\pm$ 0.0149	0.0180 $\pm$ 0.0028	0.1017 $\pm$ 0.0035
	CDMA	0.9553 $\pm$ 0.0000	0.4727 $\pm$ 0.0000	0.5015 $\pm$ 0.0000	0.1944 $\pm$ 0.0000	0.8114 $\pm$ 0.0000	0.2071 $\pm$ 0.0000	0.3607 $\pm$ 0.0000
	MotifCC	0.9712 $\pm$ 0.0098	0.7224 $\pm$ 0.0598	0.6394 $\pm$ 0.0425	0.7333 $\pm$ 0.0014	0.9433 $\pm$ 0.0032	0.7147 $\pm$ 0.0003	0.5478 $\pm$ 0.0002
	MOGC	0.9759 $\pm$ 0.0000	0.8463 $\pm$ 0.0081	0.9036 $\pm$ 0.0000	<b>0.8196</b> $\pm$ 0.0000	0.9570 $\pm$ 0.0008	0.7754 $\pm$ 0.0000	0.5855 $\pm$ 0.0000
$M_5^*$	Motif_SC	0.8255 $\pm$ 0.0000	0.5264 $\pm$ 0.0000	0.5065 $\pm$ 0.0000	0.0037 $\pm$ 0.0000	0.1490 $\pm$ 0.0000	0.0082 $\pm$ 0.0000	0.0019 $\pm$ 0.0000
	EdMot_SC	0.8419 $\pm$ 0.0336	0.3671 $\pm$ 0.1539	0.8015 $\pm$ 0.0006	0.2215 $\pm$ 0.0327	0.2858 $\pm$ 0.0070	0.0223 $\pm$ 0.0069	0.0906 $\pm$ 0.0147
	MWLP	0.9068 $\pm$ 0.0013	0.7283 $\pm$ 0.0137	0.5151 $\pm$ 0.0001	0.7796 $\pm$ 0.0059	0.3941 $\pm$ 0.0592	0.8218 $\pm$ 0.0002	0.6391 $\pm$ 0.0061
	MOSC	0.7619 $\pm$ 0.0784	0.6245 $\pm$ 0.0057	0.8190 $\pm$ 0.0000	0.0017 $\pm$ 0.0059	0.3585 $\pm$ 0.0248	0.0225 $\pm$ 0.0004	0.1124 $\pm$ 0.0002
	CDMA	0.9613 $\pm$ 0.0000	0.4533 $\pm$ 0.0000	0.5114 $\pm$ 0.0000	0.2365 $\pm$ 0.0000	0.7871 $\pm$ 0.0000	0.2037 $\pm$ 0.0000	0.3584 $\pm$ 0.0000
	MotifCC	0.9635 $\pm$ 0.0120	0.7585 $\pm$ 0.0459	0.7052 $\pm$ 0.0996	0.7312 $\pm$ 0.0021	0.9400 $\pm$ 0.0038	0.7145 $\pm$ 0.0003	0.5477 $\pm$ 0.0001
	MOGC	0.9806 $\pm$ 0.0000	0.8507 $\pm$ 0.0000	0.9021 $\pm$ 0.0000	0.7204 $\pm$ 0.0000	0.9114 $\pm$ 0.0101	0.7710 $\pm$ 0.0000	0.5377 $\pm$ 0.0000
Multiple motif	MOGC_ $M_3^3$ - $M_3^2$	0.9847 $\pm$ 0.0060	0.8548 $\pm$ 0.0068	<b>0.9110</b> $\pm$ 0.0000	0.7959 $\pm$ 0.0000	<b>0.9615</b> $\pm$ 0.0009	0.7865 $\pm$ 0.0216	0.5412 $\pm$ 0.0000
	MOGC_ $M_3^3$ - $M_4^*$	0.9771 $\pm$ 0.0000	0.8530 $\pm$ 0.0037	0.9095 $\pm$ 0.0000	0.8048 $\pm$ 0.0000	0.9568 $\pm$ 0.0009	0.7866 $\pm$ 0.0000	0.5750 $\pm$ 0.0000
	MOGC_ $M_3^3$ - $M_4^*$ - $M_5^*$	0.9844 $\pm$ 0.0000	0.8519 $\pm$ 0.0062	0.9095 $\pm$ 0.0000	0.8066 $\pm$ 0.0000	0.9568 $\pm$ 0.0009	0.7869 $\pm$ 0.0000	0.5656 $\pm$ 0.0085

higher-order and lower-order graph, then labels of isolated nodes are achieved by the label propagation on the original edge-based graph. While in our method, the label partitions of isolated and nonisolated nodes are realized within a optimization function, such that they can promote each other. Finally, when motif  $M_3^2$  is adopted, the accuracy of MOGC is further improved than that using motif  $M_3^3$ . Specially, our method has higher value of all measurements than other methods on seven datasets. This might be the fact that the density of hypergraph using motif  $M_3^2$  is larger than those using motif  $M_3^3$ , only few  $M_3^2$  based hypergraphs suffer from fragmentation issue.

#### 7.4.2. Results of 4-node Motifs and 5-node Motifs

In this subsection, we show the performances using 4-node and 5-node motifs. In the experiment, we select the top one 4-node and 5-node motif generated from mFinder3 to test our proposed method. Concretely, according to section 3, we firstly run software mFinder3 to find top one motif, then construct 4-node and 5-node motif-based adjacency matrix according to algorithm 1 in [29]. Finally, we conduct comparison experiments on seven datasets using 4-node motif and 5-node motif. For 4-node motif, we show the top one 4-node motif for seven datasets in Table. 5 and its corresponding visualization in Fig. 4, the top one 4-node motif of six datasets (football, polbooks, Cora, email-Eu-core, Citeseer, Pubmed) are  $M_4^1$ , that of polblogs is  $M_4^2$ . The top one 5-node motif and its corresponding figure for seven datasets are also shown in Table. 5 and Fig. 4. The results of all higher-order graph clustering methods are shown in Table. 3 and Table. 4, MOGC with  $M_4^*$  or  $M_5^*$  mean that both edge-based graph and top one 4-node or 5-node based hypergraphs are utilized in Algorithm 1.

As indicated by Table. 3, we can know that the performance of MOGC is better than other six higher-order graph clustering methods for almost all datasets,

Table 4: NMI Results on seven real datasets (mean $\pm$ std).

	dataset	football	polbooks	polblogs	Cora	email-Eu-core	Citeseer	Pubmed
edge	SC	0.9242 $\pm$ 0.0000	0.5422 $\pm$ 0.0261	0.0029 $\pm$ 0.0000	0.3928 $\pm$ 0.0000	0.6983 $\pm$ 0.0065	0.3701 $\pm$ 0.0000	0.1568 $\pm$ 0.0000
	Ncut	0.2435 $\pm$ 0.0135	0.3544 $\pm$ 0.0388	0.4166 $\pm$ 0.0261	0.0114 $\pm$ 0.0037	0.2389 $\pm$ 0.0055	0.0718 $\pm$ 0.0089	0.0002 $\pm$ 0.0001
	NMF	0.9199 $\pm$ 0.0085	0.5247 $\pm$ 0.0127	0.7147 $\pm$ 0.0000	0.3740 $\pm$ 0.0173	0.7005 $\pm$ 0.0053	0.2255 $\pm$ 0.0100	0.1522 $\pm$ 0.0062
	AP	0.6534 $\pm$ 0.0295	0.3546 $\pm$ 0.0182	0.2106 $\pm$ 0.0029	0.3694 $\pm$ 0.0022	0.5402 $\pm$ 0.0081	0.3263 $\pm$ 0.0029	0.1637 $\pm$ 0.0357
	N2VKM	0.9267 $\pm$ 0.0000	0.5787 $\pm$ 0.0000	0.5501 $\pm$ 0.0000	0.4643 $\pm$ 0.0001	0.7026 $\pm$ 0.0000	0.2498 $\pm$ 0.0001	0.2986 $\pm$ 0.0000
$M_3^3$	Motif_SC	0.9242 $\pm$ 0.0075	0.5531 $\pm$ 0.0452	0.0041 $\pm$ 0.0000	0.1550 $\pm$ 0.0000	0.6498 $\pm$ 0.0066	0.0774 $\pm$ 0.0000	0.0026 $\pm$ 0.0000
	EdMot_SC	0.9242 $\pm$ 0.0000	0.5583 $\pm$ 0.0236	0.7013 $\pm$ 0.0000	0.4302 $\pm$ 0.0020	0.6765 $\pm$ 0.0067	0.2500 $\pm$ 0.0290	0.2363 $\pm$ 0.0000
	MWLP	0.7885 $\pm$ 0.0031	0.3641 $\pm$ 0.0134	0.1397 $\pm$ 0.0033	0.3302 $\pm$ 0.0015	0.1053 $\pm$ 0.0000	0.0982 $\pm$ 0.0005	0.1557 $\pm$ 0.0022
	MOSC	0.8837 $\pm$ 0.0220	0.5564 $\pm$ 0.0062	0.1799 $\pm$ 0.0000	0.0774 $\pm$ 0.0000	0.6974 $\pm$ 0.0057	0.3607 $\pm$ 0.0187	0.2022 $\pm$ 0.0438
	CDMA	0.8675 $\pm$ 0.0000	0.2000 $\pm$ 0.0000	0.1109 $\pm$ 0.0000	0.0193 $\pm$ 0.0000	0.4593 $\pm$ 0.0000	0.0350 $\pm$ 0.0000	0.0030 $\pm$ 0.0000
	MotifCC	0.8922 $\pm$ 0.0116	0.5853 $\pm$ 0.1027	0.7414 $\pm$ 0.0927	0.0290 $\pm$ 0.0058	0.5152 $\pm$ 0.0378	0.0059 $\pm$ 0.0017	0.0006 $\pm$ 0.0004
	MOGC	0.9214 $\pm$ 0.0111	0.5689 $\pm$ 0.0066	0.7074 $\pm$ 0.0000	0.2427 $\pm$ 0.0000	0.6860 $\pm$ 0.0694	0.2880 $\pm$ 0.0000	<b>0.2693</b> $\pm$ 0.0041
$M_3^2$	Motif_SC	0.8957 $\pm$ 0.0377	0.5725 $\pm$ 0.0268	0.7306 $\pm$ 0.0000	0.4355 $\pm$ 0.0000	0.6852 $\pm$ 0.0055	0.3680 $\pm$ 0.0000	0.2508 $\pm$ 0.0004
	EdMot_SC	0.9043 $\pm$ 0.0000	0.5794 $\pm$ 0.0068	0.7151 $\pm$ 0.0000	0.4355 $\pm$ 0.0000	0.6878 $\pm$ 0.0035	0.3680 $\pm$ 0.0000	0.2508 $\pm$ 0.0000
	MWLP	0.4051 $\pm$ 0.0063	0.3525 $\pm$ 0.0004	0.2324 $\pm$ 0.0000	0.3233 $\pm$ 0.0017	0.0531 $\pm$ 0.0000	0.0987 $\pm$ 0.0000	0.1564 $\pm$ 0.0014
	MOSC	0.8379 $\pm$ 0.0388	0.5578 $\pm$ 0.0055	0.7380 $\pm$ 0.0000	0.1383 $\pm$ 0.0000	0.6791 $\pm$ 0.0061	0.3458 $\pm$ 0.0105	0.2358 $\pm$ 0.0329
	CDMA	0.7811 $\pm$ 0.0000	0.3974 $\pm$ 0.0000	0.0003 $\pm$ 0.0000	0.2129 $\pm$ 0.0000	0.1288 $\pm$ 0.0000	0.1480 $\pm$ 0.0000	0.0525 $\pm$ 0.0000
	MotifCC	0.8518 $\pm$ 0.0269	0.5875 $\pm$ 0.0646	0.6995 $\pm$ 0.0707	0.0377 $\pm$ 0.0085	0.4200 $\pm$ 0.0153	0.0084 $\pm$ 0.0025	0.0007 $\pm$ 0.0003
	MOGC	<b>0.9314</b> $\pm$ 0.0414	<b>0.6058</b> $\pm$ 0.0000	0.7338 $\pm$ 0.0000	<b>0.4775</b> $\pm$ 0.0000	0.6880 $\pm$ 0.0062	0.3734 $\pm$ 0.0000	0.1756 $\pm$ 0.0011
$M_4^1$	Motif_SC	0.9003 $\pm$ 0.0000	0.5742 $\pm$ 0.0000	0.0466 $\pm$ 0.0000	0.2843 $\pm$ 0.0000	0.6936 $\pm$ 0.0000	0.0618 $\pm$ 0.0000	0.0070 $\pm$ 0.0000
	EdMot_SC	0.9043 $\pm$ 0.0000	0.5761 $\pm$ 0.0000	0.1371 $\pm$ 0.0691	0.4021 $\pm$ 0.0078	0.6975 $\pm$ 0.0012	0.1213 $\pm$ 0.0377	0.0609 $\pm$ 0.0002
	MWLP	0.7692 $\pm$ 0.0031	0.5349 $\pm$ 0.0142	0.1046 $\pm$ 0.0040	0.3605 $\pm$ 0.0011	0.4488 $\pm$ 0.0011	0.3308 $\pm$ 0.0006	0.1517 $\pm$ 0.0005
	MOSC	0.8744 $\pm$ 0.0173	0.5688 $\pm$ 0.0055	0.7187 $\pm$ 0.0218	0.2593 $\pm$ 0.0000	0.6893 $\pm$ 0.0061	0.0287 $\pm$ 0.0025	0.1428 $\pm$ 0.0037
	CDMA	0.8602 $\pm$ 0.0000	0.1830 $\pm$ 0.0000	0.0158 $\pm$ 0.0000	0.0171 $\pm$ 0.0000	0.4525 $\pm$ 0.0000	0.0212 $\pm$ 0.0000	0.0093 $\pm$ 0.0000
	MotifCC	0.8883 $\pm$ 0.0290	0.5787 $\pm$ 0.1062	0.7025 $\pm$ 0.0653	0.0283 $\pm$ 0.0087	0.5029 $\pm$ 0.0199	0.0045 $\pm$ 0.0011	0.0005 $\pm$ 0.0004
	MOGC	0.9043 $\pm$ 0.0000	0.5841 $\pm$ 0.0093	0.7136 $\pm$ 0.0000	0.4628 $\pm$ 0.0010	0.6988 $\pm$ 0.0041	0.3493 $\pm$ 0.0000	0.1877 $\pm$ 0.0000
$M_5^1$	Motif_SC	0.8789 $\pm$ 0.0000	0.4346 $\pm$ 0.0000	0.4051 $\pm$ 0.0000	0.0400 $\pm$ 0.0000	0.5166 $\pm$ 0.0000	0.0610 $\pm$ 0.0000	0.0024 $\pm$ 0.0000
	EdMot_SC	0.8943 $\pm$ 0.0172	0.3723 $\pm$ 0.0933	0.7050 $\pm$ 0.0008	0.3821 $\pm$ 0.0132	0.6136 $\pm$ 0.0044	0.0406 $\pm$ 0.0206	0.1710 $\pm$ 0.0047
	MWLP	0.6222 $\pm$ 0.0043	0.4324 $\pm$ 0.0131	0.1222 $\pm$ 0.0020	0.3357 $\pm$ 0.0048	0.2148 $\pm$ 0.0125	0.3349 $\pm$ 0.0013	0.1532 $\pm$ 0.0038
	MOSC	0.8567 $\pm$ 0.0416	0.5124 $\pm$ 0.0048	0.7287 $\pm$ 0.0000	0.1378 $\pm$ 0.0000	0.6692 $\pm$ 0.0111	0.0316 $\pm$ 0.0016	0.1562 $\pm$ 0.0001
	CDMA	0.8725 $\pm$ 0.0000	0.1814 $\pm$ 0.0000	0.0830 $\pm$ 0.0000	0.0314 $\pm$ 0.0000	0.4060 $\pm$ 0.0000	0.0153 $\pm$ 0.0000	0.0003 $\pm$ 0.0000
	MotifCC	0.8660 $\pm$ 0.0336	0.5288 $\pm$ 0.0821	0.7113 $\pm$ 0.1615	0.0244 $\pm$ 0.0042	0.5356 $\pm$ 0.0239	0.0053 $\pm$ 0.0015	0.0003 $\pm$ 0.0002
	MOGC	0.9032 $\pm$ 0.0000	0.5815 $\pm$ 0.0000	0.7120 $\pm$ 0.0000	0.3897 $\pm$ 0.0000	0.6032 $\pm$ 0.0077	0.1518 $\pm$ 0.0038	0.1845 $\pm$ 0.0000
Multiple motif	MOGC_ $M_3^3$ - $M_3^2$	0.9242 $\pm$ 0.0127	0.5881 $\pm$ 0.0135	<b>0.7373</b> $\pm$ 0.0000	0.4717 $\pm$ 0.0000	<b>0.7029</b> $\pm$ 0.0061	<b>0.3878</b> $\pm$ 0.0100	0.1764 $\pm$ 0.0000
	MOGC_ $M_3^3$ - $M_4^1$	0.9134 $\pm$ 0.0000	0.5866 $\pm$ 0.0072	0.7342 $\pm$ 0.0000	0.4416 $\pm$ 0.0000	0.6957 $\pm$ 0.0033	0.3694 $\pm$ 0.0000	0.1914 $\pm$ 0.0000
	MOGC_ $M_3^3$ - $M_4^1$ - $M_5^1$	0.9193 $\pm$ 0.0000	0.5753 $\pm$ 0.0116	0.7342 $\pm$ 0.0000	0.4325 $\pm$ 0.0000	0.6962 $\pm$ 0.0049	0.3642 $\pm$ 0.0000	0.1718 $\pm$ 0.0053

which demonstrates the effectiveness of our method. Moreover, compared to the result of MOGC with  $M_3^*$ , having more nodes in a motif does not lead to better performance. In most cases, the highest accuracy is achieved with  $M_3^2$ , the reason may be the noise in motif with a large number of nodes degrades the performance.

#### 7.4.3. Results of Multiple Motifs

Since our method can utilize the information from lower-order structure and multiple higher-order structures, we conduct experiments to show the performance using edges and multiple motifs simultaneously. It is impossible to enumerate all the combination of all motifs with different number of nodes, so we test the combination of the top one 3-node, 4-node and 5-node motifs shown in Table. 5, the top one 3-node motif is  $M_3^3$  for all datasets. The results are shown in Table. 3 and Table. 4, MOGC- $M_3^3$ - $M_3^2$  indicates that edge, motif  $M_3^3$  and motif  $M_3^2$  are utilized in Algorithm 1, MOGC- $M_3^3$ - $M_4^*$  means that edge, motif  $M_3^3$  and top-1 4-node motif  $M_4^*$  are used, MOGC- $M_3^3$ - $M_4^*$ - $M_5^*$  means that edge, motif  $M_3^3$ , top one 4-node and 5-node motif are used.

As indicated by Table. 3 and Table. 4, compared with other higher-order methods, our method can achieve better results by intergrating multiple higher-order structures. For example, in Citeseer dataset, there are 1255 isolated nodes in  $M_3^3$  motif-based hypergraph, while there are no isolated nodes in  $M_3^2$  motif-based hypergraph. The NMI result of MOGC- $M_3^3$ - $M_3^2$  is about 0.13 higher than EdMot\_SC with  $M_3^3$ . As for the hypergraph of motif  $M_3^2$ , even though hypergraph fragmentation does not happen, our method still achieves 0.02 higher than EdMot\_SC in terms of NMI. For Cora dataset, highest rand index result is achieved by MOGC- $M_3^3$ - $M_4^*$ - $M_5^*$  with edge and multiple motifs. Similar analysis can be made for other datasets.

Table 5: Top one of 3-node, 4-node, 5-node motifs generated by mfinder

dataset	football	polbooks	polblogs	Cora	email-Eu-core	Citeseer	Pubmed
3-node motif	$M_3^3$	$M_3^3$	$M_3^3$	$M_3^3$	$M_3^3$	$M_3^3$	$M_3^3$
4-node motif	$M_4^1$	$M_4^1$	$M_4^2$	$M_4^1$	$M_4^1$	$M_4^1$	$M_4^1$
5-node motif	$M_5^1$	$M_5^2$	$M_5^2$	$M_5^3$	$M_5^2$	$M_5^3$	$M_5^3$

### 7.5. Adaptive Node-level Weights Analysis

The polbooks dataset is chosen to illustrate the performance of adaptive weights  $\mathbf{A}$ , the network in polbooks contains 105 nodes grouped into 3 clusters. The 1st-13th nodes belong to 1st cluster, the 14th-62nd nodes belong to 2nd cluster, and the 63th-105th nodes are in 3rd cluster. Fig. 6 shows the weights  $\mathbf{A}$  of each motif (including lower-order structure, motif  $M_3^3$  and motif  $M_3^2$ ) for each node, it is apparent that the contribution of structures are different to different nodes. We calculate the average weight for edge,  $M_3^3$  and  $M_3^2$ , they are 0.1784, 0.2532, and 0.5684 respectively, the average weight of  $M_3^2$  is higher than others. Moreover, it is shown that Motif\_SC with  $M_3^2$  has better performance than Motif\_SC with  $M_3^3$  and SC in Table.3 and Table. 4, this results validate that the obtained  $\mathbf{A}_{:,j}$  obtained by MOGC is reasonable.

To further demonstrate the performance of adaptive node-level weight, we checked two typical nodes marked by red square and green circle. The red square is the 59th node with  $\mathbf{A}_{59,1} = 0.3920$ ,  $\mathbf{A}_{59,2} = 0$ ,  $\mathbf{A}_{59,3} = 0.6080$ . Fig. 5(a) shows the corresponding adjacent weight of other nodes connected to 59th node, it is shown that 59th node becomes a isolated node without connectivity with other nodes under motif  $M_3^3$ . From Fig. 5(a), we can conclude that 59th node belongs to the 2nd cluster, nodes from the same cluster have higher similarity with 59th node than others from different clusters according to  $\mathbf{A}_{edge}$  and  $\mathbf{A}_{M_3^2}$ , so both  $\mathbf{A}_{edge}$  and  $\mathbf{A}_{M_3^2}$  contribute to the clustering of the 59th node. However, Fig. 5(a) also shows that the 59th node has denser within-cluster connectivity with  $M_3^2$  than that with edge, so  $\mathbf{A}_{M_3^3}$  can provide more accurate information to the cluster of 59th node. This result indicates that the weight of motif  $M_3^3$  would be larger than

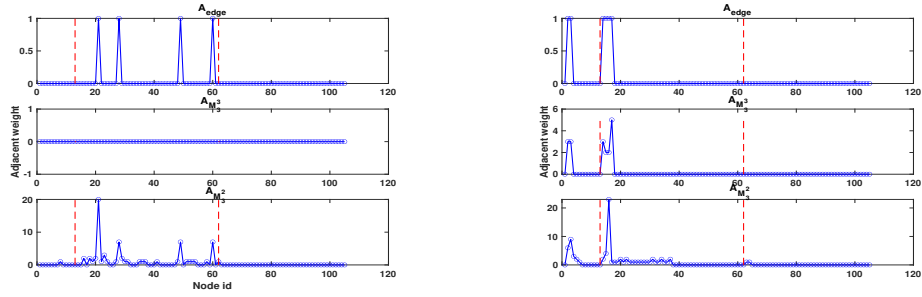
that of edge, which is consistent with calculated  $\mathbf{\Lambda}$ . The green circle is the 1st node with  $\mathbf{\Lambda}_{1,1} = 0.5060$ ,  $\mathbf{\Lambda}_{1,2} = 0.4940$ ,  $\mathbf{\Lambda}_{1,3} = 0$ . Fig. 5 (b) shows the corresponding adjacent weight of other nodes connected to 1st node. The 1st node belongs to first cluster. As can be seen, 1st node has connections with other nodes from 1st cluster and 2nd cluster. Moreover, nodes from 2nd cluster have more connectivity with larger weights with 1st node under motif  $M_3^2$ , which is not helpful to the correct partition. So it is acceptable that our method assigns 0 to the weight of motif  $M_3^2$  for 1st node. For lower-order structure and motif  $M_3^3$ , nodes both from 1st cluster and 2nd cluster have connections with 1st node according to  $\mathbf{A}_{edge}$  and  $\mathbf{A}_{M_3^3}$ , so it is reasonable that similar weights are assigned to these two motifs.

### 7.6. Parameter Analysis

Theoretically, the parameter  $\alpha$  is a trade-off parameter for smooth regularization term, an extremely small  $\alpha$  leads to an extremely sparse  $\mathbf{\Lambda}$  and an extremely large  $\alpha$  leads to a  $\mathbf{\Lambda}$  with almost identical entries. Between two extremas, we obtain suitable solutions. We use polblogs as an example to test. Fig. 7 shows the NMI value of MOGC with edge,  $M_3^3$  and  $M_3^2$  with  $\alpha$  within the range of  $[0,15]$ . It is shown that the optimal  $\alpha$  locates within  $[2,3]$ . When  $\alpha$  is small, i.e.,  $\alpha = 0.1$ , the average calculated weights for  $\mathbf{\Lambda}_{:,edge}$ ,  $\mathbf{\Lambda}_{:,M_3^3}$  and  $\mathbf{\Lambda}_{:,M_3^2}$  are 0.0969, 0.1307, 0.7724. However, when  $\alpha$  is larger, i.e.,  $\alpha = 15$ , the weight of three motifs are 0.1357, 0.1355, 0.7288, a more smooth solution for  $\mathbf{\Lambda}$  would be obtained. This results validates the setting of  $\alpha$  should be neither too small nor too large.

## 8. Conclusion

In this paper, we propose a multi-order graph clustering model (MOGC) for higher-order graph clustering. Different from the existing methods, the higher-order structures and lower-order structures are integrated at the level of node



(a) The weight of adjacency matrix for 59th node      (b) The weight of adjacency matrix for 1st node

Figure 5: The weight in adjacency matrix for nodes on polbooks dataset. The red dash lines are used to separate the nodes from different clusters.

samples with an adaptive weights learning mechanism. The proposed method can automatically adjust the contributions of different motifs to each node by the adaptive weights. This approach addresses both the hypergraph fragmentation issue and improves graph clustering accuracy by integrating information from multiple motifs at the node level. Extensive experiments have been conducted to show the effectiveness of proposed method.

In the current MOGC model, our aim is to enhance the graph clustering precise by integrating hypergraph structures from multiple motifs linearly. It is interesting to explore the nonlinear fusion of multiple motif-based hypergraphs. As a future research work, we plan to extend the multi-order graph clustering model to incorporate graph neural networks (GNNs). This extension would enable GNNs to achieve superior node representations by integrating higher-order structures from multiple motifs at the node-level nonlinearly. Consequently, this would lead to improved performances in node classification and node clustering.

## References

- [1] U. Von Luxburg, A tutorial on spectral clustering, *Statistics and computing* 17 (4) (2007) 395–416.
- [2] L. Huang, C.-D. Wang, H.-Y. Chao, A harmonic motif modularity approach for multi-layer network community detection, in: *2018 IEEE International Conference on Data Mining (ICDM)*, IEEE, 2018, pp. 1043–1048.

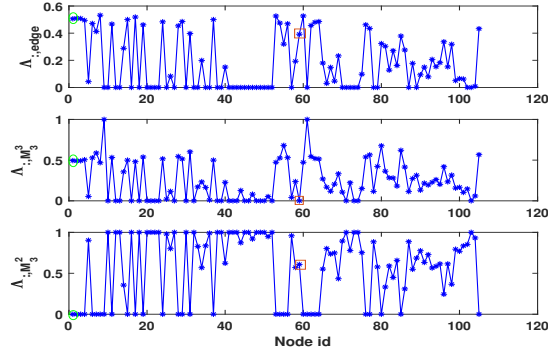


Figure 6: The weight  $\mathbf{\Lambda}$  of each motif for each node on the polbooks dataset. From top to bottom, three figures correspond to the weight of edge, motif  $M_3^3$ , motif  $M_3^2$  for each node respectively.

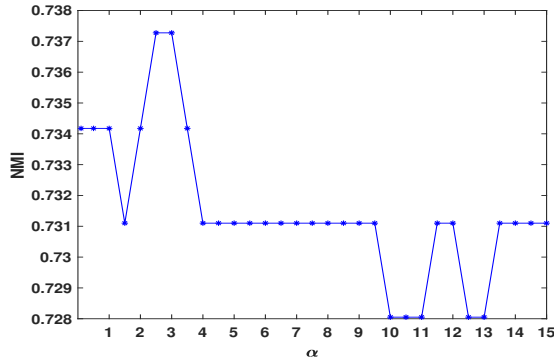


Figure 7: Sensitivity of  $\alpha$  based on polblogs dataset. Each value is the average value of 20 trials in terms of NMI.

- [3] C. E. Tsourakakis, J. Pachocki, M. Mitzenmacher, Scalable motif-aware graph clustering, in: Proceedings of the 26th International Conference on World Wide Web, 2017, pp. 1451–1460.
- [4] A. R. Benson, D. F. Gleich, J. Leskovec, Higher-order organization of complex networks, Science 353 (6295) (2016) 163–166.
- [5] P.-Z. Li, L. Huang, C.-D. Wang, J.-H. Lai, Edmot: An edge enhancement approach for motif-aware community detection, in: Proceedings of the 25th

- ACM SIGKDD international conference on knowledge discovery & data mining, 2019, pp. 479–487.
- [6] P.-Z. Li, L. Huang, C.-D. Wang, J.-H. Lai, D. Huang, Community detection by motif-aware label propagation, *ACM Transactions on Knowledge Discovery from Data (TKDD)* 14 (2) (2020) 1–19.
- [7] R. Milo, S. Shen-Orr, S. Itzkovitz, N. Kashtan, D. Chklovskii, U. Alon, Network motifs: simple building blocks of complex networks, *Science* 298 (5594) (2002) 824–827.
- [8] P. Pons, M. Latapy, Computing communities in large networks using random walks, in: *International symposium on computer and information sciences*, Springer, 2005, pp. 284–293.
- [9] D. Cai, X. He, J. Han, T. S. Huang, Graph regularized nonnegative matrix factorization for data representation, *IEEE transactions on pattern analysis and machine intelligence* 33 (8) (2010) 1548–1560.
- [10] F. Wang, C. Zhang, Label propagation through linear neighborhoods, *IEEE Transactions on Knowledge and Data Engineering* 20 (1) (2007) 55–67.
- [11] B. J. Frey, D. Dueck, Clustering by passing messages between data points, *science* 315 (5814) (2007) 972–976.
- [12] V. D. Blondel, J.-L. Guillaume, R. Lambiotte, E. Lefebvre, Fast unfolding of communities in large networks, *Journal of statistical mechanics: theory and experiment* 2008 (10) (2008) P10008.
- [13] S. Cao, W. Lu, Q. Xu, Deep neural networks for learning graph representations, in: *Proceedings of the AAAI conference on artificial intelligence*, Vol. 30, 2016.

- [14] L. Hagen, A. B. Kahng, New spectral methods for ratio cut partitioning and clustering, *IEEE transactions on computer-aided design of integrated circuits and systems* 11 (9) (1992) 1074–1085.
- [15] J. Shi, J. Malik, Normalized cuts and image segmentation, *IEEE Transactions on pattern analysis and machine intelligence* 22 (8) (2000) 888–905.
- [16] A. Arenas, A. Fernandez, S. Fortunato, S. Gomez, Motif-based communities in complex networks, *Journal of Physics A: Mathematical and Theoretical* 41 (22) (2008) 224001.
- [17] H. Yin, A. R. Benson, J. Leskovec, D. F. Gleich, Local higher-order graph clustering, in: *Proceedings of the 23rd ACM SIGKDD international conference on knowledge discovery and data mining*, 2017, pp. 555–564.
- [18] P. Zhao, gsparsify: Graph motif based sparsification for graph clustering, in: *Proceedings of the 24th ACM International on Conference on Information and Knowledge Management*, 2015, pp. 373–382.
- [19] P. Li, H. Dau, G. Puleo, O. Milenkovic, Motif clustering and overlapping clustering for social network analysis, in: *IEEE INFOCOM 2017-IEEE Conference on Computer Communications*, IEEE, 2017, pp. 1–9.
- [20] C. Li, X. Guo, W. Lin, Z. Tang, J. Cao, Y. Zhang, Multiplex network community detection algorithm based on motif awareness, *Knowledge-Based Systems* 260 (2023) 110136.
- [21] L. Huang, H.-Y. Chao, Q. Xie, Mumod: A micro-unit connection approach for hybrid-order community detection, in: *Proceedings of the AAAI conference on artificial intelligence*, Vol. 34, 2020, pp. 107–114.

- [22] X. Wu, C.-D. Wang, P. Jiao, Hybrid-order stochastic block model, in: Proceedings of the AAAI Conference on Artificial Intelligence, Vol. 35, 2021, pp. 4470–4477.
- [23] Y. Gao, X. Yu, H. Zhang, Graph clustering using triangle-aware measures in large networks, *Information Sciences* 584 (2022) 618–632.
- [24] Y. Ge, P. Peng, H. Lu, Mixed-order spectral clustering for complex networks, *Pattern Recognition* 117 (2021) 107964.
- [25] X. Wu, C.-D. Wang, J.-Q. Lin, W.-D. Xi, S. Y. Philip, Motif-based contrastive learning for community detection, *IEEE Transactions on Neural Networks and Learning Systems* (2024).
- [26] M. Jha, C. Seshadhri, A. Pinar, Path sampling: A fast and provable method for estimating 4-vertex subgraph counts, in: Proceedings of the 24th international conference on world wide web, 2015, pp. 495–505.
- [27] P. Wang, J. C. Lui, D. Towsley, J. Zhao, Minfer: A method of inferring motif statistics from sampled edges, in: 2016 IEEE 32nd international conference on data engineering (ICDE), IEEE, 2016, pp. 1050–1061.
- [28] N. Kashtan, S. Itzkovitz, R. Milo, U. Alon, Efficient sampling algorithm for estimating subgraph concentrations and detecting network motifs, *Bioinformatics* 20 (11) (2004) 1746–1758.
- [29] H. Zhao, X. Xu, Y. Song, D. L. Lee, Z. Chen, H. Gao, Ranking users in social networks with motif-based pagerank, *IEEE Transactions on Knowledge and Data Engineering* 33 (5) (2019) 2179–2192.
- [30] G. H. Golub, C. F. Van Loan, *Matrix computations*, JHU press, 2013.

- [31] A. Ng, M. Jordan, Y. Weiss, On spectral clustering: Analysis and an algorithm, *Advances in neural information processing systems* 14 (2001).
- [32] F. Wang, T. Li, X. Wang, S. Zhu, C. Ding, Community discovery using non-negative matrix factorization, *Data Mining and Knowledge Discovery* 22 (3) (2011) 493–521.
- [33] A. Grover, J. Leskovec, node2vec: Scalable feature learning for networks, in: *Proceedings of the 22nd ACM SIGKDD international conference on Knowledge discovery and data mining*, 2016, pp. 855–864.
- [34] W. M. Rand, Objective criteria for the evaluation of clustering methods, *Journal of the American Statistical association* 66 (336) (1971) 846–850.
- [35] A. Amelio, C. Pizzuti, Is normalized mutual information a fair measure for comparing community detection methods?, in: *Proceedings of the 2015 IEEE/ACM international conference on advances in social networks analysis and mining 2015*, 2015, pp. 1584–1585.